비탄성 비뉴톤성 유체의 애눌라다이 팽창

서용석·김광웅

한국과학기술연구원 고분자 공정 연구실
(1989년 8월 8일 접수)

Annular Die Swelling of Inelastic Non-Newtonian Fluids

Yongsok Seo and Kwang Ung Kim

Polymer Processing Laboratory, Korea Institute of Science and Technology P.O. Box 131, Cheongryang, Seoul, Korea

(Received August 8, 1989)

요 약

유한요소법을 이용하여 애눌라다이 팽창현상을 수치 해석학적으로 분석하였다. 이 보고는 계속적인 연구의 일부로써 비탄성 비뉴토니안 유체인 지수법칙형의 유체에 대한 모사이다. 이 지수법칙형의 유체는 간단하나 고분자 공정 연구에 많이 쓰이는 구성식으로써, 분석결과는 환형압출체의 두께는 지수법칙 지수에 비례하여 증가하였다. 높은 전단응력 감소유체의 경우 두께는 증가하지 않고 감소하였다. 비등온 유체 및 여러 다른 형태의 압출형에 대한 수치해석 결과도 예시하였다.

Abstract—Annular extrudate swell is studied using a finite element method. Power-law fluid was simulated, which has a simple form but is important for polymer processing analysis. The result shows that thickness swelling increases with power-law index. For highly shear thinning fluids, extrudate thickness was contracted rather than swollen. Nonisothermal case is also studied.

Keywords: Inelastic fluid/Extrudate swell/Finite element method/Nonisothermal fluid/Annular flow

INTRODUCTION

Some time ago, a finite element method was used for the analysis of the annular die swelling problem [1], which does not accept any simple reasonable anlaytical solution due to its complicated geometry originating from two free surface, positions of which are not known *a priori*. This report presents a partial result of continuous study of annular die swelling problem.

As well known, the dimensions of annular jet depend on the swelling ratios, which are influenced by extrusion conditions, rheological properties of polymeric fluids, and die geometry. In this article, for a non-Newtonian fluid, power-law fluid model was used to investigate the effect of shear thickening or shear thinning on annular extrudate swell.

MATHEMATICAL FORMULATION AND A FINITE ELEMENT SCHEME

The mathematical description of the steady fluid motion is assumed to be given by the following equations:

$$\nabla \cdot V = 0 \qquad (1)$$

(continuity equation)

$$\rho V \cdot \nabla V = \rho f + \mathrm{div}\,\sigma = -\nabla p + \rho f + \nabla \cdot \tau \qquad (2)$$

(momentum equation)

Here the fluid was assumed to be incompressible. In these equations, V represents the fluid velocity vector, ρ the density, f the body force vector per unit mass, τ deviatoric stress tensor, σ total stress tensor ($= -pI + \tau$), p pressure.

For the power-law fluid deviatoric stress tensor is expressed as

$$\tau = \eta A^{(1)} \qquad (3)$$

Here $A^{(1)}$ is the first Rivlin-Ericksen tensor, defined by

$$A^{(1)} = 2D = \nabla V + (\nabla V)^T = L + L^T \qquad (4)$$

where D is the symmetric part of the velocity gradient L (∇V)

Substituting (4) into (3) yields the following equation for τ

$$\tau = \eta (L + L^T) \qquad (5)$$

where η is a function of the strain rate $\dot{\gamma}$ and temperature. Generally this can be presented as

$$\eta = \eta_0 (\dot{\gamma})^{n-1} \exp(-b \cdot (T - T_0)) \qquad (6)$$

Here η_0 is a material parameter, b is a constant, T_0 is a reference temperature, and n is the power index. The transport of thermal energy in the fluid is described by

$$\rho C_p V \cdot \nabla T = S + \nabla \cdot (k \cdot \nabla T) + \tau : D \qquad (7)$$

(energy equation)

where C_p is the specific heat, S is the volumetric heat source, k is the thermal conductivity tensor. With the suitable boundary conditions, these four equations (Eqs. (1),(2),(5) and (7)) form the basis of the finite element method used in this study. Using the variational staterment for these equations implicitly included in conjunction with a finite element interpolation for the independent variables V, p and T yields the standard finite element equations. Since the finite element scheme used in this study has been fully described elsewhere [2], we don't repeat lengthy and complicated derivation and only mention briefly the main features of this scheme. Basically the finite element method code used here is designed for steady state, incompressible, two dimensional (plane or axisymmetric without torsion) fluid problems. It is based on the Galerkin descritisation procedure, solving simultaneously equations (1),(2),(5) and (7) in their full nonlinear forms. To solve nonlinear terms, iteration was done until converagence occurs using Newton-Raphson iteration method or successive substitution method [2].

FREE SURFACE ITERATIONS AND A PROBLEM DESCRIPTION

In a free surface problem, such as die swelling problem, an additional source of nonlinearity is present since the location of the free surface is not known *a priori*. Consider the fluid emerging from a die into the atmosphere as shown in Fig 1. If the shear stress due to the surrounding air can be ignored, the free surface condition is equivalent to setting the shear stress to zero and the normal stress to the ambrient pressure (generally taken as zero). Also in this class of problems, in addition to the nonlinearity due to unknown free surface location, a singularity at die exit is present since the fluid velocity changes from zero (no-slip condition on the wall before emerging from the die) to non-zero value (the no-shear condition after exiting from the die) in an infinitesimal distance. This is also the situation in what so called a stick-slip problem, except the free surface condition.

The shape of the free surface is calculated by means of an iterative procedure [3]. Let's consider the case of an annular die in Fig. 1 with two free surface S_1 and S_2 described by the equations
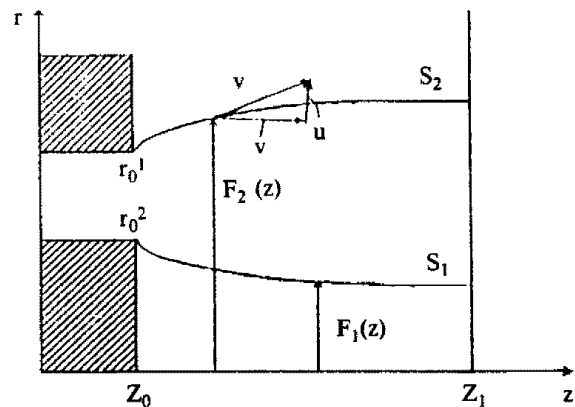

Fig. 1. Description of the free surface problem

$$r^1 = F_1(z), \quad r^2 = F_2(z) \quad z_0 \leq z \leq z_1 \qquad (8)$$

Since the free surface is also a stream surface, we must have

$$\frac{dF_i(z)}{dz} = \frac{u}{v} \{z, F_i(z)\} \quad F_i(z_0) = r_0^i \quad i = 1,2 \qquad (9)$$

where u and v are the radial and axial velocities respectively, and r_0^i are the fixed radius positions at the exit. The iterative procedure starts from cylindrical surfaces on which vanishing contact forces are imposed; new surfaces are defined by the equations

$$\frac{dF_i^{n+1}(z)}{dz} = \frac{u}{v} \{z, F_i^n(z)\}, \quad F_i^{n+1}(z_0) = r_0^i \quad i = 1,2 \,(10)$$

Here F_i^n means n th iterated free surfaces. Integrating equation (10) gives

$$F_i^{n+1} - F_i^0 (=r_0^i) = \int_{z_0}^{z_1} \frac{u}{v} \{z, F_i^n(z)\} dz \quad i = 1,2 \qquad (11)$$

These are integrated by means of Simpson's rule and generally five or six iterations were enough to produce converged free surface positions, but sometimes it needs more iterations.

The basic qualitative aspects of the annular jet swelling problem are quite similar to those for the capillary or plane die swelling problems. However, as mentioned before, a major difference is the absence of an axis or plane of symmetry and this necessitates a consideration of the entire flow field bounded by the two surfaces of the annular channel; in another words, we should solve two free surface problem.

The other thing to be mentioned is that for annular jet swelling, we can define three different swelling ratios, inside diameter swelling (S_i), outside diameter swelling (S_o), and thickness swelling (S_t) as follows;

$$S_o = \frac{[R_{out}^{final}(z_\infty) - R_{out}^{initial}(z_\infty)]}{R_{out}^{initial}(z_\infty)} = \frac{R_o^f}{R_o^i} - 1.$$

$$S_i = \frac{[R_{in}^{initial}(z_\infty) - R_{in}^{final}(z_\infty)]}{R_{in}^{initial}(z_\infty)} = 1. - \frac{R_i^f}{R_i^i}$$

$$S_t = \frac{[R_{out}^{final}(z_\infty) - R_{in}^{final}(z_\infty)]}{[R_{out}^{initial}(z_\infty) - R_{in}^{initial}(z_\infty)]} - 1. \qquad (12)$$

where R_{in} means the inside radius, R_{out} is the outside radius, $z\infty$ is far downstream, initial means the in-

itial position before free surface iteration, final means the final position after free surface iteration. These swelling ratios are related to each other. If R_o^i and R_i^i are 1 and k respectively in dimensionless values, they can be presented as follows;

$$S_o = R_o^f - 1$$
$$S_i = 1 - (R_i^f / k)$$
$$S_t = [R_o^f - R_i^f] / [1 - k] - 1. \quad \text{or}$$
$$S_t = [(1 + S_o) - (1 - S_i)^*k] / [1 - k] - 1. \qquad (13)$$

The dimensionless values used were $R_o = 1.$, $R_i = k.$ ($= 0.5$), $v_{avg} = 1.$, $\rho = 1.$ E-5 and $\eta = 1.$

As we said, "power-law" fluid was used, which has a simple form of constitutive equation but is important in many industrial polymer processing operations. For simple shearing motion, the viscosity depends on shear rate nonlinearly and it is presented as in equation (6). In equation (6), $\dot{\gamma}$ is presented in another way as (II) 0.5 generally. II is the second invariant of the rate of deformation tensor. In equation (6), when $n = 1$, we recover a Newtonian fluid behaviour and when $n < 1$, the flow is pseudo-plastic (or shear thinning) and when $n > 1$, it is dilatent (or shear thickening). As explained by Tanner, et al [4], stability consideration forbids a negative value of n, because the shear stress should not decrease with increasing shear rate. So $n = 0$ represents the lower limit for n. In this case ($n = 0$), we have a plug flow in a die.

The computations were done using the same grid that was used for the Newtonian fluid case for $k = 0.5$ (104 elements, 8×13 mesh. [1]). The problem sketch is shown in Fig. 2(a) and its grid is shown in Fig. 2(b) for a straight die of $k = 0.5$. The upstream and downstream lengths were taken eight times of die gap to get the converged shapes and to exclude die exit di-
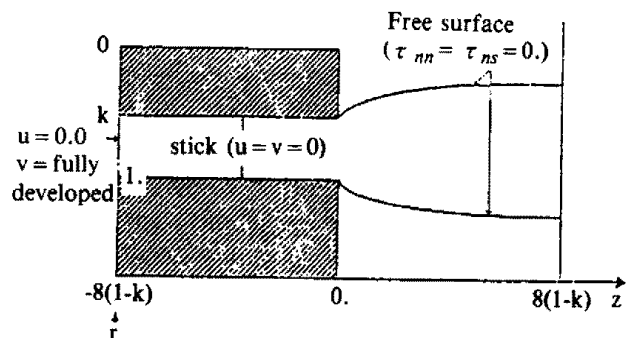
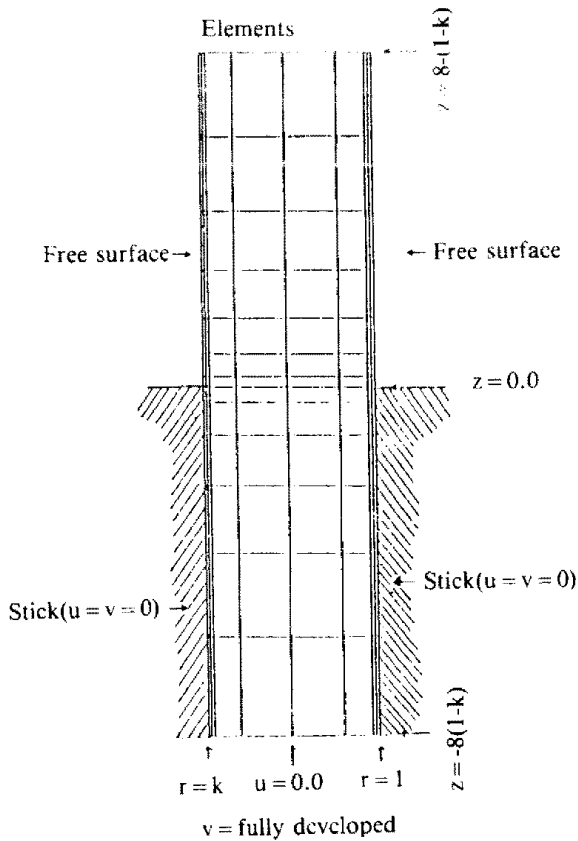Fig. 2(a). Annular die swelling problem sketch

Fig. 2(b). Finite element grid for a die swelling problem

sturbances. Through this study, nine node Lagrangian elements were used. Boundary conditions on the free surfaces and solid walls are identical for all fluids- we assume the normal and tangential stress vanish on the free surfaces and the fluid sticks to solid walls. One thing that should be mentioned is that the entry boundary condition at far upstream is more complex than for a Newtonian fluid. The annular velocity profiles of a power-law fluid is more difficult to obtain as shown in a paper by Fredrickson and Bird [5]. It is easy to show that the shear stress component has the general form $Ar + B/r$; thus for a fluid with power-law index n, we have following relationship

$$\eta_0 |\dot{\gamma}|^n = \pm (Ar + B/r) \tag{14}$$

This equation can be solved separately for two ranges, $\dot{\gamma} \leq 0$ and $\dot{\gamma} \geq 0$, to obtain solutions that join at some radius λ where $A\lambda + B/\lambda = 0$. A,B and two intergration constants can be obtained by specifying the flow rate, no-slip conditions at the walls and continuity of velocity at $r = \lambda$. However, this requires a considerable computational work. As an alteration, boundary condition and flow rate of a Newtonian fluid were applied at far upstream

of the die, then the fluid will have non-Newtonian fluid velocity profile marching through the fluid path. So it is necessary to use a longer domain than for a Newtonian fluid to give enough space developing a non-Newtonian velocity profile. It was observed from numerical result that eight times length of die gap was enough for the power-law fluid case.

RESULTS AND DISCUSSION

Dimensional analysis shows that without gravity and surface tension, the isothermal extrudate swell is a function of power-law index, n, in the creeping flow limit. Table 1 presents computed results for this case when $Re = 10^{-5}$. The thickness swells more with increasing n. We can expect this easily due to the shearing in a die and the velocity arrangement at downstream [6]. The fluid moves outward more for shear thickening fluid. The thickness swelling with power-law index n is presented in Fig. 3. From Fig. 3, we can see that the thickness swelling ratio increases almost linearly when n is greater than 0.1. Also a linearized approximation line is presented in Fig. 3 when the power-law index n is larger than 0.2. It is presented

$$S_t = 0.223n - 0.077 \tag{15}$$

When n is 1.4, S_t reaches as much as 23.25%. So a shear thickening fluid, we can expect a relatively large thickness swelling, although it is still not comparable to a real polymeric fluid thickness swelling ratio. Overall thickness swelling behaviour is similar to that of capillary die swelling [4]. However, for shear thinning fluid (n < 1) the thickness swelling is not so large, and since most polymeric fluids or melts have a value of n between 0.4 and 0.6, as well known, we

Table 1. Annular jet swelling with power-law index.

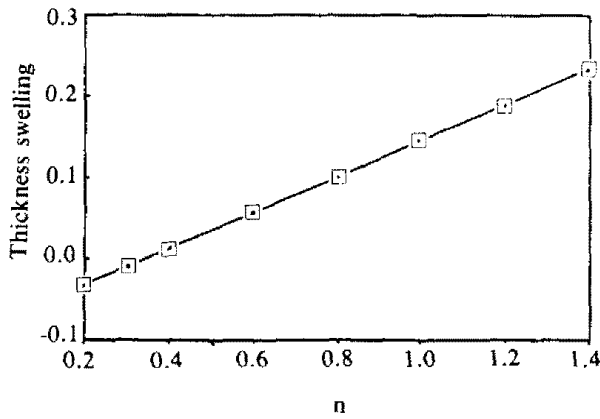| n	S_o %	S_i %	S_t %
1.4	16.21	-9.164	23.25
1.2	12.22	-5.242	19.19
1.	8.6	-2.6	14.6
0.8	5.38	-0.28	10.47
0.6	2.73	0.363	5.813
0.4	0.676	-0.218	1.103
0.3	- 0.13	-0.845	- 1.103
0.2	- 0.755	-1.767	- 3.277

Fig. 3. Variation of thickness swelling vs power-law index, n
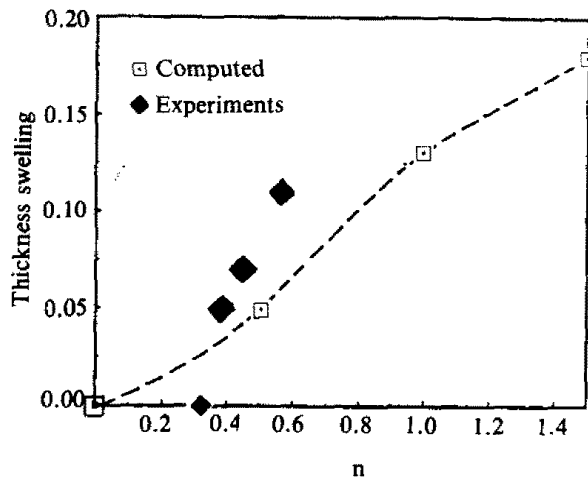
Fig. 4. Swelling of creeping power-law jets from capillary as a function of power-law index, n[4]

curred to annular jet when n is smaller than 0.4 seems due to fluid nature and its stick boundary condition at the wall. The more the fluid becomes shear thining (in another words the smaller the n value becomes), the more its axial velocity profile becomes flat in the die, but never totally flat because the stick boundary condition at the die wall requires zero velocity there. If the fluid is totally inviscid then it is the same as one flowing inside of the die with complete slip condition, which yields a plug flow. This case was studied by Silliman and Scriven [9], and as we expect, admitting perfect slip (a plug flow) does not produce any swelling at all. For very small values of n, however, shearing is confined to regions near the wall and a large portion of the fluid has a higher velocity than the average axial velocity. Hence, the fluid element does not deform much after emerging from a die. This can be explained in terms of velocity changes after die exit. Fig. 5 shows the axial velocity change along the fluid path when n is 0.2 (and the data is presented in Table 2). As we can see, the axial velocity does not change much after extrusion except near die lips. Fluid elements near die lips are under a pulling force, and to balance it, elements near the fluid center are under compression. But owing to the almost flat velocity profile in the fluid, the compression is distributed evenly across the fluid thickness. Hence, there is not large pushing from

say that non-Newtonian, inelastic behaviour of polymeric melt or fluid is not the cause of their large extrudate swell. It sould be pointed out that when the power-law index is less than 0.4 in Table 1, the thickness swelling ratio becomes negative, which means thickness contraction rather than swelling. Tanner and his co-workers [4,7,8] said die swelling for a capillary flow decreases with decreasing power-law index and no swelling occurrs when power-law index has its minimum value, i,e., zero. Fig. 4 shows their computational result and also Wale's experimental result [4]. In Fig. 4, experimental result shows that thickness swelling reaches 1 when n is near 0.3, while their computational result decreases smoothly to zero with small value of n. In Fig. 4 there is not any thickness reduction in Tanner et al's computational result. The thickness reduction oc-
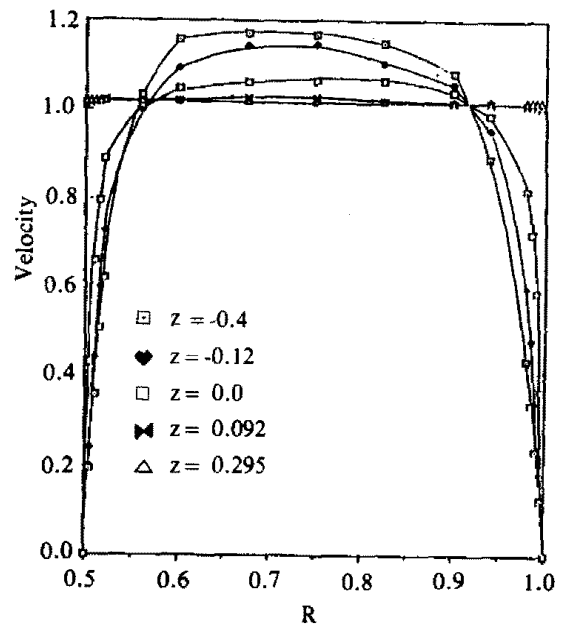

Fig. 5. Axial velocity profiles along fluid path when n equal to 0.2

Table 2. Axial velocity along fluid path when n = 0.2

Node No.	R	$z = -0.4$	$z = -0.12$	$z = 0.0$	R	$z = 0.092$	$z = 0.295$
1	0.5	0.	0.	0.	0.5087	1.007	1.021
2	0.505	0.192	0.24	0.425	0.514	1.014	1.0213
3	0.51	0.356	0.435	0.658	0.518	1.018	1.0214
4	0.515	0.496	0.595	0.795	0.523	1.02	1.0215
5	0.52	0.614	0.728	0.889	0.528	1.021	1.0216
6	0.56	1.035	1.0	1.013	0.567	1.021	1.0216
7	0.6	1.16	1.094	1.052	0.605	1.023	1.0217
8	0.675	1.171	1.143	1.066	0.678	1.031	1.0217
9	0.75	1.17	1.148	1.068	0.75	1.029	1.0217
10	0.825	1.152	1.16	1.067	0.823	1.021	1.0217
11	0.9	1.086	1.06	1.044	0.895	1.019	1.0217
12	0.94	0.893	0.955	0.993	0.934	1.018	1.0217
13	0.98	0.431	0.595	0.823	0.973	1.017	1.0217
14	0.985	0.338	0.474	0.722	0.978	1.016	1.0217
15	0.99	0.236	0.337	0.583	0.983	1.013	1.0216
16	0.995	0.123	0.18	0.364	0.987	1.007	1.0215
17	1.	0.	0.	0.	0.9923	1.007	1.021

Table 3. Nonisothermal swelling of power-law fluids when Pe = 1. No viscous heat dissipation

a) shear thinning fluid, n = 0.5

β	0.25			0.75		
Nu	S_o	S_i	S_t	S_o	S_i	S_t
0.	1.54	0.08	3.18	1.54	0.08	3.18
5.	1.32	0.05	2.7	0.9	-0.04	1.8
20.	1.35	0.06	2.75	0.97	-0.05	1.89

b) shear thickening fluid, n = 1.4

β	0.25			0.75		
Nu	S_o	S_i	S_t	S_o	S_i	S_t
0.	16.21	-9.164	23.25	16.21	-9.164	23.25
5.	15.12	-8.5	21.74	13.58	-6.9	20.24
20.	15.29	-8.6	21.97	14.02	-7.18	20.86

fluid center. Even though the pushing from the center is small, the stretching at die lips would be relatively large compared to compression at the center. This makes the fluid contract after extrusion. When n is less than 0.1, it took very long computational time to get a converged solution. So it was not attempted any more, but it is deemed that there might be a minimum position of power-law index, n, where thickness reaches its minimum beyond that wall slip effect becomes more dominant to make the fluid thickness increase to be 1 at n equal to zero (perfect slip).

As a next step, non-isothermal annular extrudate swell of a power-law fluid was investigated. Recently Huynh [10] reported the computational results of a non-isothermal capillary extrusion for power-law fluids. According to his results, increasing the temperature dependency parameter of viscosity, β ($= b^*(T_o-T\infty)$), always brought increased swelling due to viscous heat dissipation. The effect was stronger at high values of the power-law index n, and for shear thinning fluids (n < 1) there was hardly any variation at all in swelling with changing β. His result was for a high Pe (Peclet number) problem. Here a similar problem was solved with convection boundary condition and temperature dependent viscosity. Since the annular die swelling
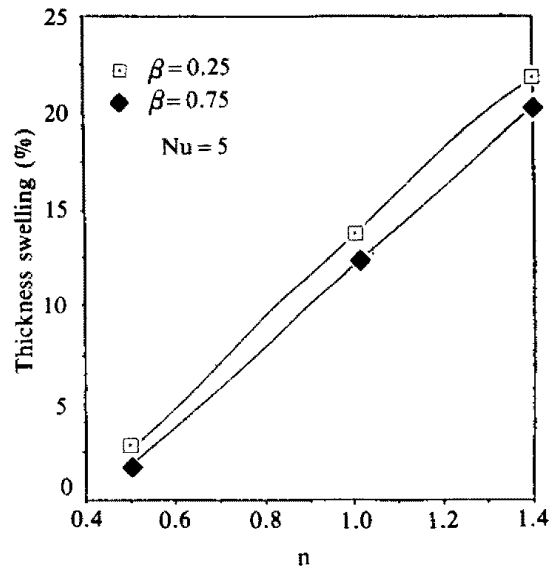

Fig. 6. Thickness swelling with power-law index without viscous heat dissipation

problem of a nonisothermal Newtonian fluid was investigated else where [2], we will briefly represent nonisothermal case of power-law fluids. Briefly speaking, the result was similar to nonisothermal Newtonian jet swelling and no significant difference was found at all. Table 3 summarizes the results when Pe is 1 and no heat dissipation occurs. As a reference, the thickness swelling, S_t, is plotted against power-law index n in Fig. 6 for two different values of temperature dependence parameter for viscosity ($\beta = 0.25$ and 0.75). Although the values are different, we can see that the general trend is the
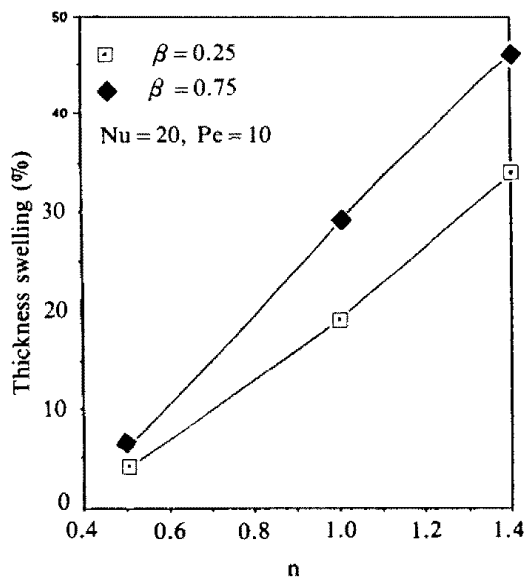
Fig. 7. Thickness swelling with power-law index with viscous heat dissipation

Table 4. The effect of die geometry for power-law fluids

Die	30° converging			30° diverging		
n	0.6	1.	1.4	0.6	1.	1.4
S_o %	-1.95	1.02	5.24	18.68	34.78	66.31
S_i %	20.25	35.14	40.8	-32.41	-56.36	-105.7
S_t %	5.79	16.31	24.7	-2.98	0.74	4.13

same as a Newtonian fluid case. For nonisothermal swelling problem with viscous heat dissipation, even though the amount of heat dissipation is different with different values of n, the general trend is the same as a Newtonian fluid case, so it is not repeated here. As a reference, some results are presented in Fig. 7 when $Pe = 1$, $Nu = 20$ and $\beta = 0.25$ and 0.75. As seen before, large swelling is possible for a nonisothermal shear thickning fluid.

To investigate the effect of the die geometry (See Seo and Wissler [1] for details about the effect of die geometry on Newtonian annular jet swelling problems), calculations were done for 30° converging and diverging dies for power-law fluids. For power-law fluids, we expect that a higher value of n will produce large swelling due to large shearing. Table 4 summarizes the results which agrees with our expectations. A shear thinning fluid even experiences thickness reduction due to hoop stress and small shearing. These results were obtained using an ex-

tended domain $-6 \leq z \leq 6$ to get a converged jet shape.

CONCLUSION

As a part of continuous study, annular extrudate swell for inelastic viscous fluid was investigated using a finite element method. Their general behavior was similar to that of a Newtonian fluid. Thickness swelling ratio was increased for more shear thickening fluids in all cases whereas highly shear thinning fluid showed a contraction rather than swelling. As we expect, shear rate dependent viscosity does not give enough thickness swelling comparable to that of polymeric melts or solutions. Thickness contraction for a highly shear thinning fluid is deemed because of problem conditions. Further results for viscoelastic fluid will be reported elsewhere.

NOMENCLATURE

$A^{[1]}$: the first Rivlin-Ericksen tensor
b : a constant in the fluid viscosity exponential term
C_p : the specific heat
D : the symmetric part of the velocity gradient
f : the body force vector per unit mass
F_i : free surface position ($i = 1$ for inners surface, 2 for outer surface)
I : identity tensor
II : the second invarianrt of the rate of deformation tensor
k : the thermal conductivity tensor
k : dimensionaless inner surface radius
L : the velocity gradient tensor
L^T : transpose of the velocity gradient tensor
n : power-law index
V : the fluid velocity vector
p : pressure
r : radial axis in the cylindrical coordinate
r^1 : inner surface radial position
r^2 : outer surface radial position
R : fluid surface radius
S : the volumetric heat sources
S_i : inside diameter swelling ratio
S_o : outside diameter swelling ratio
S_t : thickness swelling ratio
T : fluid temperature
T_o : reference temperature
T_∞ : environment temperature

u   : radial direction fluid velocity component

v   : axial direction fluid velosity component

z   : vertical axis in cylindrial coordinate

Greek Letter

β : dimensionless parameter ($= b^*(T_o-T\infty)$)

$\dot{\gamma}$: rate of strain

η_o : parameter of the fluid viscosity

η : the fluid viscosity

λ : the fluid position where $\dot{\gamma}$, the rate of strain is zero

ρ : the fluid density

σ : total strees tensor

τ : deviatoric stress tensor

REFERENCES

1. Y. Seo. and E.H. Wissler, *J. Applied Polym. Sci.* 37, 1159 (1989).

2. Y. Seo. and E.H. Wissler, in press *Polym. Eng. Sci.* (1989).

3. M.J. Crochet. and R. Keunings *J. Non-Newtonian Fluid Mech,* 7, 199 (1980).

4. R.I. Tanner., R.E. Nickel. and Bilger, R.W. *Comp. Meth. Appl. Mech. Eng.* 6, 15 (1975).

5. A.G. Fredrickson. and R.B. Bird. *Ind. Eng. Chem.* 50, 347 (1958).

6. Y. Seo. PhD Dissertation University of Texas at Austin (1987).

7. Tanner, R.I. *J. Non-Newtonian Fluid Mech.* 7, 265 (1980).

8. R.J. Fischer. M. Denn. and R.I. Tanner. *Ind. Eng. Chem. Fluid.* 19, 195 (1980).

9. Sillinan, W.J. and Scriven, L.E. *J. Comp. Phys.* 34, 287 (1980).

10. B.P.J. Huynh. *J. Non-Newtonian Fluid Mech.* 13, 1 (1982).